Isoliensinine induces cervical cancer cell cycle arrest and apoptosis by inhibiting the AKT/GSK3α pathway

HONG-LI LI[1,2*], YAN CHENG[1,3*], ZI-WEI ZHOU[1,3], HUI-ZHI LONG[1,3],
HONG-YU LUO[1,3], DAN-DAN WEN[1], LIN CHENG[4] and LI-CHEN GAO[1,3]

[1]Department of Pharmacy, Cancer Institute, Phase I Clinical Trial Centre, Changsha Central Hospital Affiliated to
University of South China, School of Pharmacy, University of South China, Changsha, Hunan 410000;
[2]School of Life Science, Hunan University of Science and Technology, Xiangtan, Hunan 411201;
[3]Hunan Provincial Key Laboratory of Tumor Microenvironment Responsive Drug Research Affiliated to School of Pharmacy,
University of South China, Hengyang, Hunan 421001; [4]State Key Laboratory of Ophthalmology,
Zhongshan Ophthalmic Center, Sun Yat-sen University, Guangzhou, Guangdong 510060, P.R. China

Abstract. Isoliensinine is a bis-benzylisoquinoline alkaloid that can be isolated from the lotus *Nelumbo nucifera* Gaertn. It has been reported to exert a variety of anti-cancer properties. In the present study, the potential effects of isoliensinine on cervical cancer Siha, HeLa, Caski and C33A cell lines were investigated by using Cell Counting Kit-8 (CCK-8), flow cytometry, western blotting and reverse transcription-PCR (RT-PCR) to measure cell proliferation, the cell cycle and apoptosis, in addition to elucidating the underlying molecular mechanism. Protein levels of p21, CDK2, Cyclin E, Mcl-1, cleaved Caspase-9, AKT, phosphorylated-AKT, glycogen synthase kinase (Gsk)3α, PTEN, and mRNA levels of p21, p15, p27, CDK2, CDK4, Cyclin E, Cyclin D, Gsk3α, Gsk3β and PTEN were measured. Molecular docking assays were used to calculate the strength of binding of isoliensinine to AKT using AutoDock 4.0. Isoliensinine was found to induce cell cycle arrest at the G_0/G_1 phase by upregulating p21 expression and downregulating CDK2 and cyclin E in cervical cancer cells. In addition, in previous research, isoliensinine promoted cell apoptosis by downregulating myeloid-cell leukemia 1 expression and activating caspase-9. Upstream, isoliensinine significantly downregulated AKT (S473) phosphorylation and GSK3α expression in a dose- and time-dependent manner. The AKT inhibitor AKTi-1/2 enhanced the function of isoliensinine on cell cycle arrest and apoptosis through the AKT/GSK3α pathway. AutoDock analysis showed that isoliensinine can bind to the AKT protein. These findings suggest that isoliensinine can induce cervical cancer cell cycle arrest and apoptosis by inhibiting the AKT/GSK3α pathway, which represents a novel strategy for the treatment of cervical cancer.

Introduction

Cervical cancer is the fourth most frequently diagnosed cancer among women, with ∼604,000 new cases worldwide in 2020 (1). Cervical cancer can be treated surgically if detected early, but at later stages treatment options become limited and the survival rate is low (2). Persistent infection with human papillomavirus (HPV) is one of the major causes of cervical cancer (3). HPV can activate the AKT pathway to promote cell proliferation, which is one of the first steps of cervical cancer tumorigenesis (4). Accumulating evidence has shown that AKT is highly activated in cervical cancer tissues compared with that in normal tissues, which promotes cancer cell proliferation (5,6). Therefore, reversing AKT hyperactivation can potentially restrain cell proliferation, thereby improving the efficacy of cervical cancer treatment to increase the survival rate of patients.

AKT is composed of a regulatory domain, kinase domain and a pleckstrin homology (PH) domain (6). After cells are stimulated with growth factors or other signaling molecules such as EGF and PDK1, AKT is recruited to the cell membrane, where the PH domain binds to phosphatidylinositol 3-phosphate (PI3P), which then exposes the active sites that were previously masked by the PH domain (6). AKT is predominately inactivated through dephosphorylation by PTEN (6). Activated AKT then targets downstream protein glycogen synthase kinase 3 (GSK3) to elicit physiological effects, including cell proliferation and survival (7,8). p21 has been previously reported to be negatively regulated by the AKT/GSK3 pathway to promote cell proliferation (8). In

Correspondence to: Dr Li-Chen Gao, Department of Pharmacy, Cancer Institute, Phase I Clinical Trial Centre, Changsha Central Hospital Affiliated to University of South China, School of Pharmacy, University of South China, 161 Shaoshan South Road, Changsha, Hunan 410000, P.R. China
E-mail: gonedog1224@hotmail.com; 89206346@qq.com

*Contributed equally

addition, myeloid-cell leukemia 1 (Mcl-1) can be regulated by AKT/GSK3 pathway to promote cell survival (9). AKT suppression has also been found to induce caspase-dependent death of certain cells, including but not limited to, chronic lymphocytic leukemia cells and SW620 cells (9-12). Therefore, targeting AKT as a potential treatment strategy for cancer has garnered considerable attention in this research field (13).

Isoliensinine is a bisbenzylisoquinoline alkaloid that can be isolated from the seed, fruit and germ of the lotus plant *Nelumbo nucifera* Gaertn (14-16). It has a variety of reported anticancer properties (14-16). Previous studies have reported that isoliensinine can induce apoptosis by suppressing NF-κB signaling in hepatocarcinoma cells, by activating the p38 MAPK/JNK signaling in breast cancer cells, by inducing autophagy in apoptosis-defective mouse embryonic fibroblasts and by promoting synergism with cisplatin in colorectal cancer cells (16-18). However, the potential effects of isoliensinine on cervical cancer cells and underlying molecular mechanism remain poorly understood.

In the present study, it was hypothesized that isoliensinine ay exert anticancer effects on cervical cancer, possibly by regulating AKT signaling. Therefore, the present study aimed to investigate the specific molecular mechanism involved in the physiology of cervical cancer after isoliensinine treatment. Furthermore, the efficacy of combined isoliensinine and the AKT inhibitor on cervical cancer cells was tested.

Materials and methods

Cell culture. Human cervical cancer Caski, C33A, HeLa and SiHa cells were purchased from ATCC and cultured in DMEM supplemented with 10% fetal bovine serum (FBS) and 1% penicillin/streptomycin. All cells were cultured at 37°C with 5% CO_2. DMEM, FBS and 1% penicillin/streptomycin were purchased from Biological Industries.

Reagents. Isoliensinine (98% by high performance liquid chromatography; Beijing Solarbio Science & Technology Co., Ltd.) was dissolved in DMSO to 20 mg/ml. 0.1% DMSO was used as the vehicle control for isoliensinine.

AKT inhibitor AKTi-1/2 (10 mM; cat. no. SF2784) was purchased from Beyotime Institute of Biotechnology. The Cell Counting Kit-8 (CCK-8) was purchased from Shanghai Yeasen Biotechnology Co., Ltd. The Annexin V apoptosis kit (cat. no. LHK601-020) was purchased from Beijing Jiamei Nuno Biotechnology Co., Ltd.

Primary rabbit anti-human AKT (cat. no. 4691), phosphorylated (p-)AKT (S473) (cat. no. 4060), p21 (cat. no. 2947), CDK2 (cat. no. 2546), Cyclin E1 (cat. no. 20808), GSK3α (cat. no. 4337), Mcl-1 (cat. no. 94296), cleaved caspase-9 (cat. no. 9508), and GAPDH (cat. no. 5174) antibodies and secondary antibodies were purchased from Cell Signaling Technology, Inc. Secondary antibodies included the HRP-conjugated anti-rabbit antibody (cat. no. 7074) and HRP-conjugated anti-mouse antibody (cat. no. 7076). All primary antibodies were diluted at a ratio of 1:1,000, whilst all secondary antibodies were diluted at a ratio of 1:2,000 for use in the study.

CCK-8 analysis. Human cervical cancer Siha, HeLa, Caski and C33A cells were seeded into 96-well plates at a density of

8×10^3 cells/well 1 day before isoliensinine treatment. After the cells were treated with 0, 5, 10, 15, 20 or 25 μM isoliensinine for 24 and 48 h at 37°C, DMEM (100 μl/well) containing 10 μl CCK-8 was added. The cells were then cultured at 37° for a further 2 h before absorbance was measured in each well at 450 nm. The cell viability was calculated by the formula [experimental optical density (OD) values-background OD values]/(control OD values-background OD values) x100. All experiments were performed in triplicate. The IC_{50} value was calculated by non-linear regression (curve fit) using the GraphPad Prism 8 software (GraphPad Software, Inc.). The XY drawing was first elected to create a new file and before the corresponding data were entered. The data were then converted into logarithmic format, following which 'Transform' and 'Transform X values using X=Log (X)' were selected under the 'analysis column'. Finally, 'non-linear expression (curve fit)' and 'dose-response-inhibition' were selected for the IC_{50} calculations.

Colony formation assay. Cervical cancer HeLa and C33A cells were plated into six-well plates at a density of 1×10^3 cells/well and treated with isoliensinine at concentrations of 0, 1, 2, 4 or 8 μM at 37°C, and 0.1% DMSO was used as a negative control. The media was changed after 48 h of incubation. At 10-14 days later, when colonies were present, the cervical cancer cells were fixed with 4% methanol for 20 min and stained with 0.1% gentian violet for 30 min at room temperature. Valid clones that contained >50 cells were manually counted.

Cell cycle analysis. Human cervical cancer Siha, HeLa, Caski and C33A cells were seeded in six-well culture plates at a density of 5×10^5 cells/well and then treated with isoliensinine (0-40 μM) and AKTi-1/2 (7.5 μM). After treatment with isoliensinine for 24 h at 37°C, the cells were collected in pre-cooled microcentrifuge tubes and centrifuged at 2,000 x g for 5 min at room temperature and washed once with PBS. The cells were stored at 4°C overnight after fixation with 70% ethanol. After 70% ethanol fixation, the cells were collected by centrifugation again at 2,000 x g for 5 min at room temperature, washed twice with PBS and treated with 2 μl RNase and 2 μl propidium iodide (PI). The cells were incubated at room temperature for 30 min. A total of 3×10^4 cells were collected from each sample for flow cytometry analysis using BD Accuri™ C6 software (version 1.0.264.21; BD Biosciences).

Flow cytometry analysis of cell apoptosis. Human cervical cancer Siha, HeLa, Caski and C33A cells were seeded into six-well culture plates at a density of 1×10^5 cells/well. After treatment with isoliensinine (0-40 μM) and AKTi-1/2 (7.5 μM) for 48 h at 37°C, the cells were dislodged and centrifuged at 2,000 x g for 5 min at room temperature, washed once with PBS and labeled with FITC isomer for 15 min at room temperature in the dark. Prior to flow cytometry analysis, the cells were stained with PI for 5 min and mixed at room temperature in the dark. A total of 5×10^4 cells were obtained for each sample and analyzed by flow cytometry.

During analysis, in the apoptosis diagram quadrant Q3 represents the population of early apoptotic cells whereas quadrant Q2 represents the population of late apoptotic cells. Together, these quadrants were used for quantification of apoptosis in each treatment group.

Table I. Primer sequence and amplicon sizes.

Gene	Sequence (5'→3')	Amplicon size (bp)
GAPDH	F: AGAAGGCTGGGGCTCATTT	280
	R: CCATCACGCCACAGTTTCC	
p21	F: TGGGGATGTCCGTCAGAA	474
	R: TTCCTCTTGGAGAAGATCAGC	
GSK3α	F: TGGCAGTGCAAAGCAGTTG	326
	R: GCGTTCGAGATTTGAACACCT	
GSK3β	F: TTTTGCTCGTCTCTTCCACA	311
	R: ATTGAGCAAGGGTAGAGATGG	
Cyclin E	F: CGTTCTCTTCTGTCTGTTGCA	317
	R: TACAACGGAGCCCAGAACA	
Cyclin D	F: ATGCTGAAGGCGGAGGAGA	398
	R: TGTTCAATGAAATCGTGCGG	
P15	F: GGACTAGTGGAGAAGGTGCG	243
	R: GGGCGCTGCCCATCATCATG	
P27	F: TGCAACCGACGATTCTTCTACTCAA	185
	R: CAAGCAGTGATGTATCTGATAAACAAGG	
CDK2	F: GGACGGAGCTTGTTATCGCAAAT	61
	R: CCTTGGCCGAAATCCGCTT	
CDK4	F: AGGCTTTTGAGCATCCCA	278
	R: TCCTTAGTCGTTTCGGCT	
PTEN	F: CATGACAGCCATCATCAAAG	346
	R: CTGGGAATAGTTACTCCCTT	
Bid	F: ACTGTGAGGTCAACAACGGTT	483
	R: TGTGACTGGCCACCTTCTTG	
Bad	F: TGTTCCAGATCCCAGAGTTTG	430
	R: CTTTGCCGCATCTGCGTT	
Bcl-2	F: TCAAAGTGCAGCTCCGTTT	342
	R: ACCATTCATGCTCCATCTGA	
Bax	F: CAGCTCTGAGCAGATCATGAA	420
	R: TCTTGGATCCAGCCCAACA	

GSK, glycogen synthase kinase; F, forward; R, reverse.

Reverse transcription (RT)-PCR and RT-quantitative PCR (RT-qPCR). Human cervical cancer Siha, HeLa, Caski and C33A cells were incubated with 0, 5, 10, 20 or 40 μM isoliensinine for 24 h at 37°C. Subsequently, they were dislodged and collected in pre-cooled microcentrifuge tubes at 2,000 x g for 5 min at room temperature and dissolved in TRIzol reagent (Invitrogen; Thermo Fisher Scientific, Inc.). Total RNAs were extracted and reverse transcribed into cDNAs using the RevertAid First Strand cDNA Synthesis Kit (cat. no. K1622; Thermo Fisher Scientific, Inc.). First-strand cDNA was synthesized using the temperature protocol of 65°C for 5 min, 60 min at 42°C and termination by heating at 70°C for 5 min.

Subsequent PCR was prepared using 2X Taq Master Mix (cat. no. E005-02A; Novoprotein; Jinan Protein Technology Co., Ltd.) and ran in a ProFlex PCR System (Thermo Fisher Scientific, Inc.) using the following thermocycling protocol: 94°C for 1 min for preheating, followed by 20-30 cycles at 94°C for 30 sec for denaturation, 60°C for 30 sec for annealing and 68°C for 40 sec for extension, and then a final cumulative amplification at 68°C for 10 min. GAPDH was used as the internal reference and was run for 20 cycles, whereas the target genes shown in Table I and p21, Cyclin E and CDK2 were run for 25-30 cycles. The PCR products were separated by 1% agarose gel stained with 7% GelRed (cat. no. 41003; Biotium, Inc.) and Tanon 2500 Gel Imaging System (Tanon Science and Technology Co., Ltd.) was used for imaging the gels.

For RT-qPCR, the qPCR reaction was prepared using FastStart™ Universal SYBR® Green Master Mix (Roche Diagnostics) and analyzed using an Applied Biosystems QuantStudio 3 Real-time PCR machine with the following thermocycling reactions: 1 cycle at 95°C for 60 sec; followed by 45 cycles of 95°C for 10 sec, 60°C for 10 sec and 72°C for 10 sec; then 1 cycle at 95°C for 10 sec, 65°C for 60 sec and 97°C for 1 sec. GAPDH was used as the control to evaluate mRNA expression in each sample and mRNA expression was analyzed using the $2^{-\Delta\Delta Cq}$ method [19]. The primers of CDK2, cyclin E, CDK4, Cyclin D1, p27, p15 and PTEN were designed according to previous studies [20-24] and are listed as Table I.

Western blotting. Human cervical cancer Siha, HeLa, Caski and C33A cells were seeded into 12-well culture plates at $1x10^5$ cells/well and were cultured overnight at 37˚C. After adding 0, 5, 10, 20 or 40 μM isoliensinine, AKTi-1/2 (7.5 μM) and 0.1% DMSO as control treatment for 24 h at 37˚C, the cells were washed once with PBS and dissolved in Cell Lysis Buffer for Western and IP (cat. no. P0013; Beyotime Institute of Biotechnology) supplemented with phosphatase and protease inhibitor cocktails. The cell lysates were then transferred to pre-cooled microcentrifuge tubes and centrifuged at 12,000 x g for 10 min at 4˚C.

The cells were dissolved in lysis buffer (Beyotime Institute of Biotechnology) according to the number of cells, then heated at 100˚C for 5 min and separated on a 10% gel using SDS-PAGE. Subsequently, the proteins were transferred onto PVDF membranes. The membranes were washed once for 10 min in PBS-T (PBS; 1% Tween-20) and blocked with 3% non-fat milk dissolved in PBS-T for 1 h at room temperature. The membranes were then incubated with the primary antibodies overnight at 4˚C, washed three times with PBS-T and incubated with secondary antibodies for 1.5 h at room temperature. Finally, the membranes were washed three times with PBS-T and visualized by Western Bright™ ECL HRP substrate (Advansta, Inc.).

Molecular docking. The complex models of human AKT1 (PDB ID, 6HHF) and AKT2 (PDB ID, 3D0E) were retrieved from https://www.rcsb.org/. Ligands data were shown as https://www.rcsb.org/structure/6HHF and https://www.rcsb.org/structure/3D0E. Ligands from AKT1/2 were separated following the prompt command using the AutoDock Tools software (http://mgltools.scripps.edu/downloads; version 1.5.6).

AKT1/2 docking was performed using the AutoDock 4.0 (http://autodock.scripps.edu/; version 4.0) and AutoDock Tools 1.5.6 software, whereas ligands (isoliensinine and AKTi-1/2) were drawn using the Chem3D (https://www.chemdraw.com.cn/; version 20.0) software. The selection of flexible residues (from docking center, AKT1: CYS296, AKT2: MET229) was based on previous reports (25,26). The docking center and grid box of AKT1was x=8.717, y=4.212 and z=11.536, and x=60, y=60 and z=66, respectively. The docking center and grid box of AKT2 was x=16.477, y=-34.368 and z=1.722, and x=60, y=60 and z=66. Independent docking calculations for AKT1/2 ligands were conducted with 250,000 evaluations using the Lamarckian genetic algorithm (27). The results were analyzed using the PyMol (https://pymol.org/2/; version 2.0) software.

Statistical analysis. Student's unpaired t-test and one-way ANOVA were used to compare the differences between two groups or multiple groups. Tukey's post hoc test was performed after one-way ANOVA. GraphPad Prism 8 software (GraphPad Software, Inc.) for analyzes. Data are presented as the means ± standard deviation from three independent experiments. P<0.05 was considered to indicate a statistically significant difference.

Results

Isoliensinine inhibits cell proliferation in cervical cancer cells. In the present study, the effects of isoliensinine on the proliferation of human cervical cancer cell lines C33A, Caski, HeLa and SiHa cells were assessed. Isoliensinine dose-dependently inhibited the proliferation of cervical cancer cells (Fig. 1A). Following treatment with 25 μM isoliensinine, the cell viability of C33A, Caski, HeLa and SiHa cells were decreased to 12.49, 14.91, 26.16 and 39.66 at 24 h, respectively, which decreased further to 3.2, 1.78, 3.97 and 13.13 at 48 h, respectively (Fig. 1A). In addition, the IC_{50} value was calculated to be 13.45 and 11.04 μM for HeLa at 24 and 48 h, respectively. The IC_{50} value was calculated to be 10.27 and 7.26 μM for Caski at 24 and 48 h, respectively. By contrast, the IC_{50} value was calculated to be 16.74 and 13.16 μM for SiHa at 24 and 48 h, respectively. The IC_{50} value for C33A cells was calculated to be 9.53 and 7.88 μM at 24 and 48 h, respectively.

Furthermore, after isoliensinine (10 μM) treatment for 24 and 48 h, the cell viability of HeLa and SiHa cells was markedly higher compared with that of C33A cells, whilst the viability of Caski cells was comparable with that of C33A cells (Fig. 1A). Results of colony formation assay of cervical cancer cell lines C33A and HeLa revealed that isoliensinine could significantly inhibit the proliferation of cervical cancer cells (Fig. 1B). In addition, in the colony formation assay, small doses of isoliensinine (2-8 μM) was sufficient to significantly inhibit the proliferation of cervical cancer cells, suggesting that the specific mechanism may involve changes in pharmacokinetics.

Isoliensinine induces cell cycle arrest at the G_0/G_1 phase in cervical cancer cells. To examine if the inhibitory effects of isoliensinine on proliferation was due to cell cycle arrest, the cell cycle distribution of the four cervical cancer cell lines was examined by flow cytometry. Isoliensinine treatment significantly increased G_0/G_1 cell cycle arrest in the four cervical cancer cell lines in a dose-dependent manner (Figs. 2A and B, and S1A and B). After isoliensinine treatment for 24 h, the number of cells in G_1 phase increased while those in the S and G_2 phases decreased dose-dependently (Fig. 2C). Furthermore, after 40 μM isoliensinine treatment, the percentages of C33A, Caski, HeLa and SiHa cells in G_1 phase were increased by 19.67, 14.33, 25.33 and 15.67% (Fig. 2C), respectively. By contrast, those in S phase were decreased by 7.33, 3, 10 and 5% in C33A, Caski, HeLa and SiHa cells, respectively (Fig. 2C). Those in G_2 phase were also decreased by 12.33, 11.33, 15.66 and 10.66% in C33A, Caski, HeLa and SiHa cells, respectively (Fig. 2C).

To elucidate the mechanism by which isoliensinine regulates cell cycle progression in cervical cancer cells, RT-PCR and western blotting were performed to measure the expression of cell cycle regulators (Figs. 3A and B, and S2). Isoliensinine upregulated p21 whilst downregulating CDK2 mRNA expression at the transcriptional level (Fig. 3A). Specifically, after 40 μM isoliensinine treatment, the mRNA expression of p21 were increased by 20.6-, 4.99-, 4.50- and 2.19-folds in C33A, CaSki, HeLa and SiHa cells, respectively (Fig. 3A). However, CDK2 mRNA expression was decreased by 0.48-, 0.5-, 0.41- and 0.48-folds in C33A, CaSki, HeLa and SiHa cells, respectively (Fig. 3A). Cyclin E mRNA were decreased by 0.05-, 0.07- and 0.14-folds in C33A, HeLa and SiHa cells, respectively (Fig. 3A). Changes in CDK2 and cyclin E expression were not prominent in Caski and HeLa cells on the transcriptional level (Fig. 3A). However, isoliensinine markedly reduced CDK2 and cyclin E
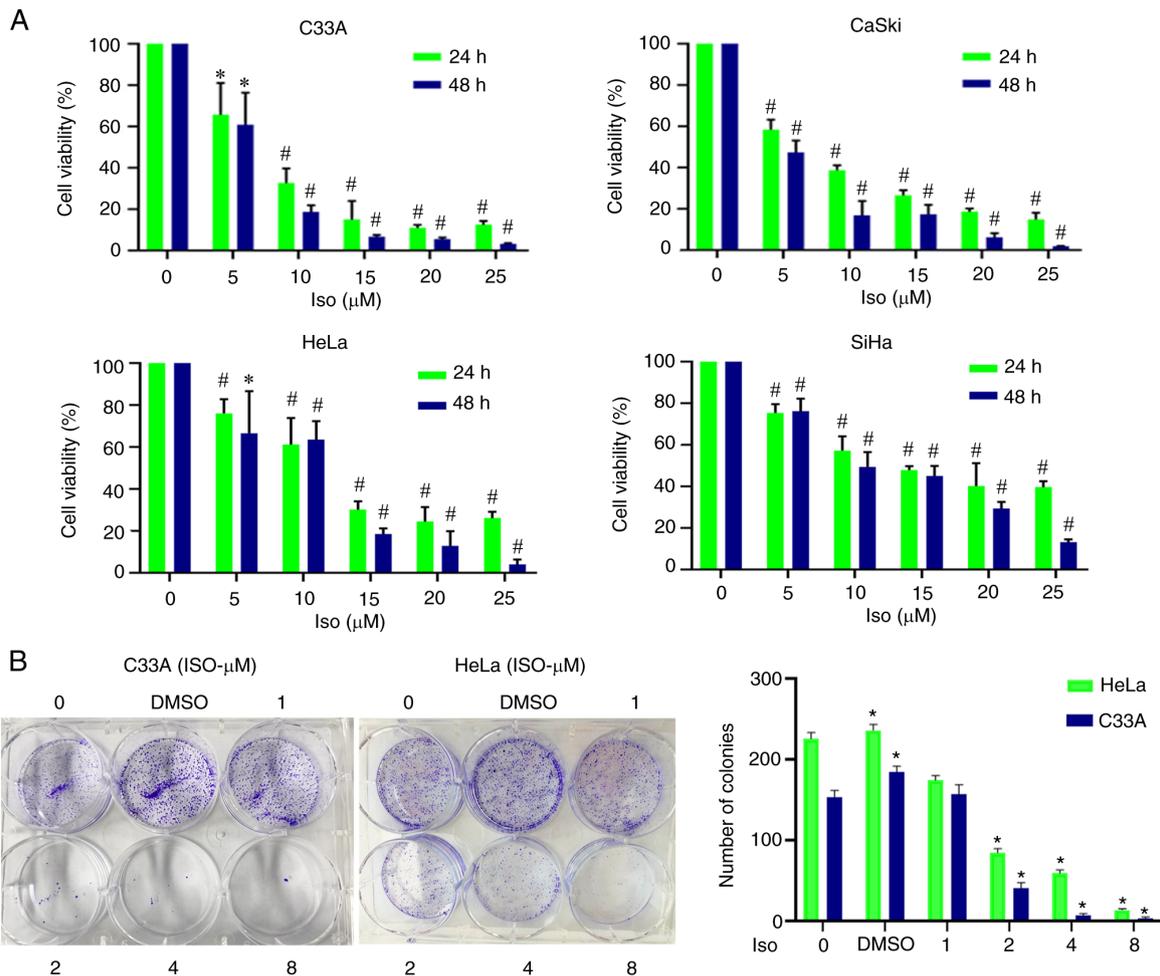
Figure 1. Isoliensinine inhibits the proliferation of cervical cancer cells. (A) Cervical cancer cell lines were exposed to 0, 5, 10, 15, 20 and 25 (μM) isoliensinine for 24 and 48 h. (B) Cervical cancer cell lines C33A and HeLa were treated with different doses of isoliensinine (0, 1, 2, 4 and 8 μM) prior to colony formation assay. *P<0.05 and #P<0.01, vs. 0. Iso, isoliensinine.

on the protein level in the four cervical cancer cells in a dose-dependent manner (Fig. 3B).

Isoliensinine induces apoptosis in cervical cancer cells. Results from apoptosis assay revealed the dose- and time-dependent induction of apoptosis by isoliensinine in the four cervical cancer cell lines (Figs. 4A-D and S3-5). After isoliensinine (40 μM) treatment for 48 h, the percentages of apoptosis for C33A, Caski, HeLa and SiHa cells were increased by 46.60, 70.35, 23.10 and 53.63%, respectively (Fig. 4B). After isoliensinine (20 μM) treatment for 72 h, the percentages of apoptosis for these cells were increased by 66.87, 59.61, 29.78 and 50.55% in C33A, Caski, HeLa and SiHa cells, respectively (Fig. 4D).

Significant changes were not observed in the expresion of mRNA in the Bcl-2 family, namely Bcl-2, Bid, Bad and Bax, according to results from RT-PCR assay (Fig. S6A). Mcl-1 was previously reported to be highly expressed in cervical cancer tissue compared with that in normal tissue and was closely associated with the apoptosis of cervical cancer HeLa cells (28,29). Mcl-1 is a major member of the Bcl-2 family that can inhibit cell apoptosis (29). Western blotting results demonstrated that isoliensinine downregulated Mcl-1 expression and activated caspase-9 in a dose-dependent manner in SiHa and HeLa cells (Fig. 4E).

Isoliensinine inhibits AKT (S473) phosphorylation and GSK3α expression in cervical cancer cells. Isoliensinine was found to inhibit AKT phosphorylation and reduce GSK3α expression in the four cervical cancer cell lines in a dose- and time-dependent manner (Fig. 5A and B). However, isoliensinine downregulated AKT (S473) phosphorylation without affecting total AKT expression (Fig. 5A). Additionally, the expression of the negative regulatory factor of AKT PTEN was also mesured by RT-PCR and western blotting. Isoliensinine did not appear to induce marked changes in PTEN expression. (Figs. S2 and S6B).

To clarify the relationship between isoliensinine and AKT, the 3D structure of isoliensinine combined with the AKT1/2 proteins was analyzed using the AutoDock assay software (Fig. 6). The docking analysis showed that the docking site of isoliensinine was similar to that of AKTi-1/2. In total, the following 14 amino acids interacted with isoliensinine in AKT1: Tyr272, Asp274, Cys296, Gln79, Val270, Lys297, Leu295, Val271, Tyr18, Glu17, Gly16, Ile19, Glu85 and Thr82 (Fig. 6C). By contrast, 11 amino acids interacted with isoliensinine in AKT2: Ala173, Thr313, Glu193, Val147, Leu296, Asp275, Lys277, His355, Tyr217, Ser476 and Lys191 (Fig. 6D). Furthermore, the binding energies of isoliensinine with AKT1 and AKT2 were -7.46 and -2.31
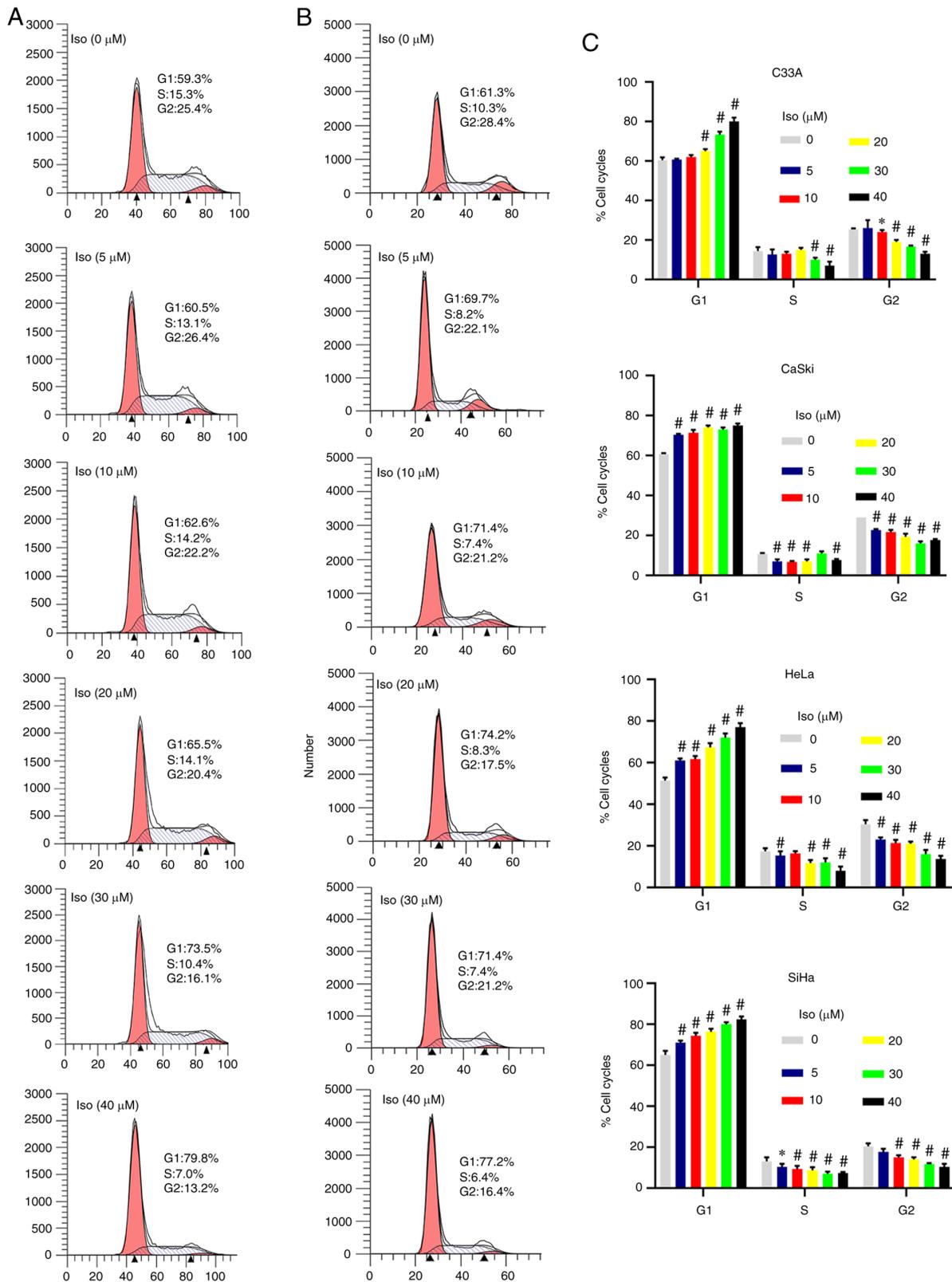
Figure 2. Isoliensinine induces G_0/G_1 phase cell cycle arrest in cervical cancer cells. Cervical cancer cells were exposed to 0, 5, 10, 20, 30 and 40 μM isoliensinine for 24 h. Cell cycle phase distribution was assessed in (A) C33A and (B) Caski cells. G_1 and G_2 are indicated by small black triangles on the x-axis. (C) Quantitative data of cervical cancer cell cycle phase distribution. Cell cycle distribution was measured by flow cytometry. *P<0.05 and $^\#$P<0.01 vs. 0 (Further data are presented in Fig. S1). Iso, isoliensinine.

kcal/mol, respectively. AKTi-1/2 presented prominent inter-actions with 13 amino acid residues in AKT1 at an affinity of -11.92 kcal/mol: Leu264, Tyr263, Ser205, Tpr80, Leu210,

Thr211, Asp292, Thr82, Gly294, Ile84, Cys296, Tyr272 and Asp274 (Fig. 6E). AKTi-1/2 docked with 12 residues in AKT2 at an affinity of -5.98 kcal/mol: Ala173, Glu171,
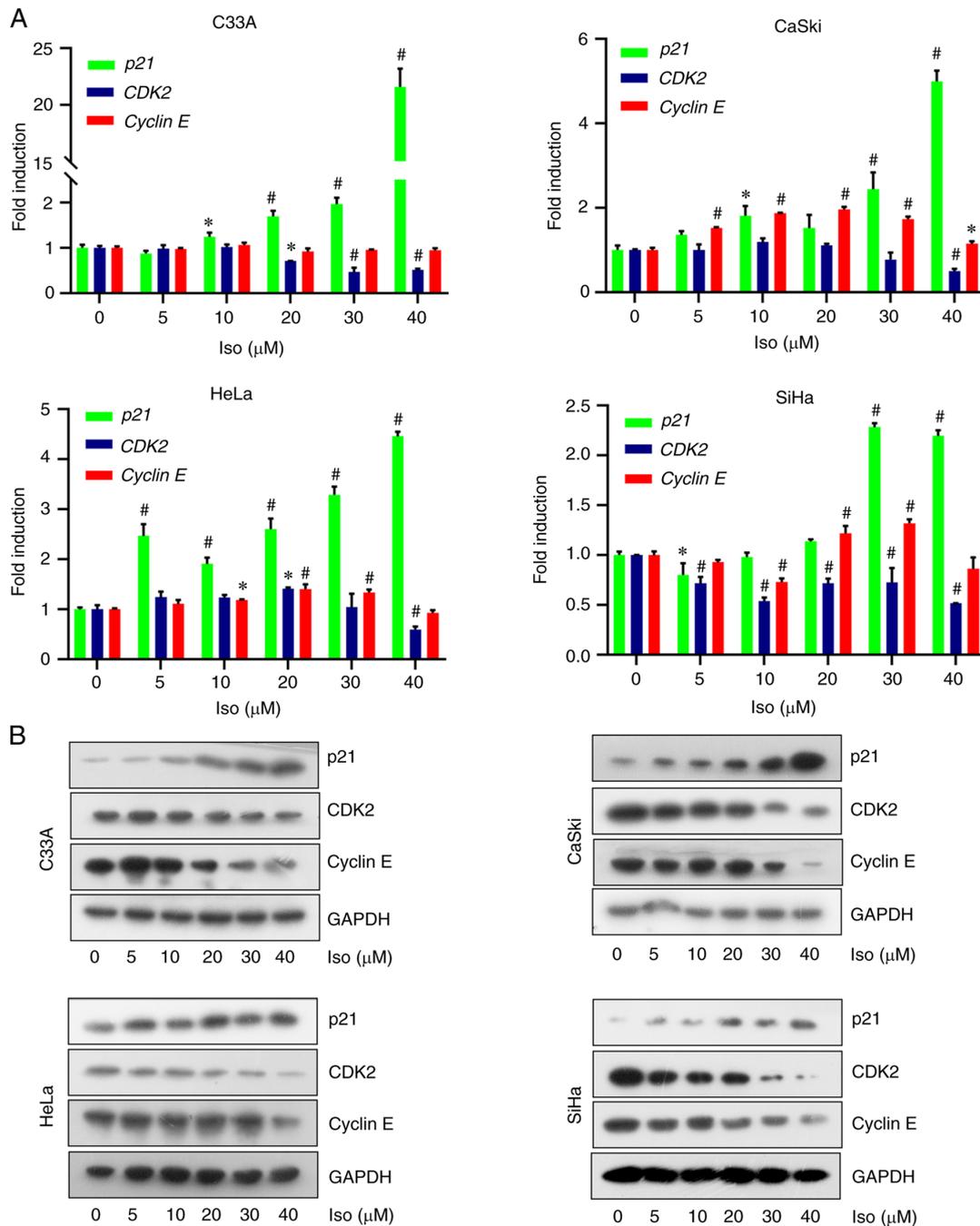
Figure 3. Isoliensinine upregulates p21 expression to induce G_0/G_1 cervical cancer cell cycle arrest. The cells were treated with 0, 5, 10, 20, 30 and 40 μM isoliensinine for 24 h. (A) Reverse transcription-quantitative PCR and (B) western blot analysis of p21, CDK2 and Cyclin E expression in HeLa and C33A cervical cancer cells. GAPDH was used as a control. Iso isoliensinine. *P<0.05 and #P<0.01 vs. 0.

His355, Glu315, Pro314, Thr313, Leu296, Asp293, His196, Glu193, Thr197 and Lys181 (Fig. 6F).

Isoliensinine induces cell cycle arrest and apoptosis through the AKT/GSK3α pathway in cervical cancer cells. To investigate whether the effects of isoliensinine on cell cycle arrest and apoptosis were similar to those of the AKT inhibitor AKTi-1/2, a series of experiments were conducted using AKTi-1/2 as a control in the four cervical cancer cell lines. According to previous studies and the IC_{50} data, 5-10 μM AKTi-1/2 was selected (30,31). On the basis of ensuring that the level of apoptosis was not too high, 7.5 μM was selected.

AKTi-1/2 was found to enhance the function of isoliensinine in inducing cell cycle arrest (Figs. 7A and B, and S7). After the combined treatment for 24 h, the percentages of C33A, Caski and HeLa cells in G_0/G_1 phase were increased by 13.16, 8 and 21.96%, respectively. Those in S phase were decreased by 4.1, 2.9 and 4.04%, respectively (Fig. 7B). In addition, those in the G_2 phase were decreased by 8.87, 5.23 and 17.73%, respectively (Fig. 7B). AKTi-1/2 also enhanced the ability of isoliensinine to induce apoptosis in cervical cancer cells (Fig. 8A-D). After the combined treatment for 48 h, the percentages of apoptotic C33A, Caski and HeLa cells were increased by 48.3, 77.46 and 10.06%, respectively (Fig. 8D).
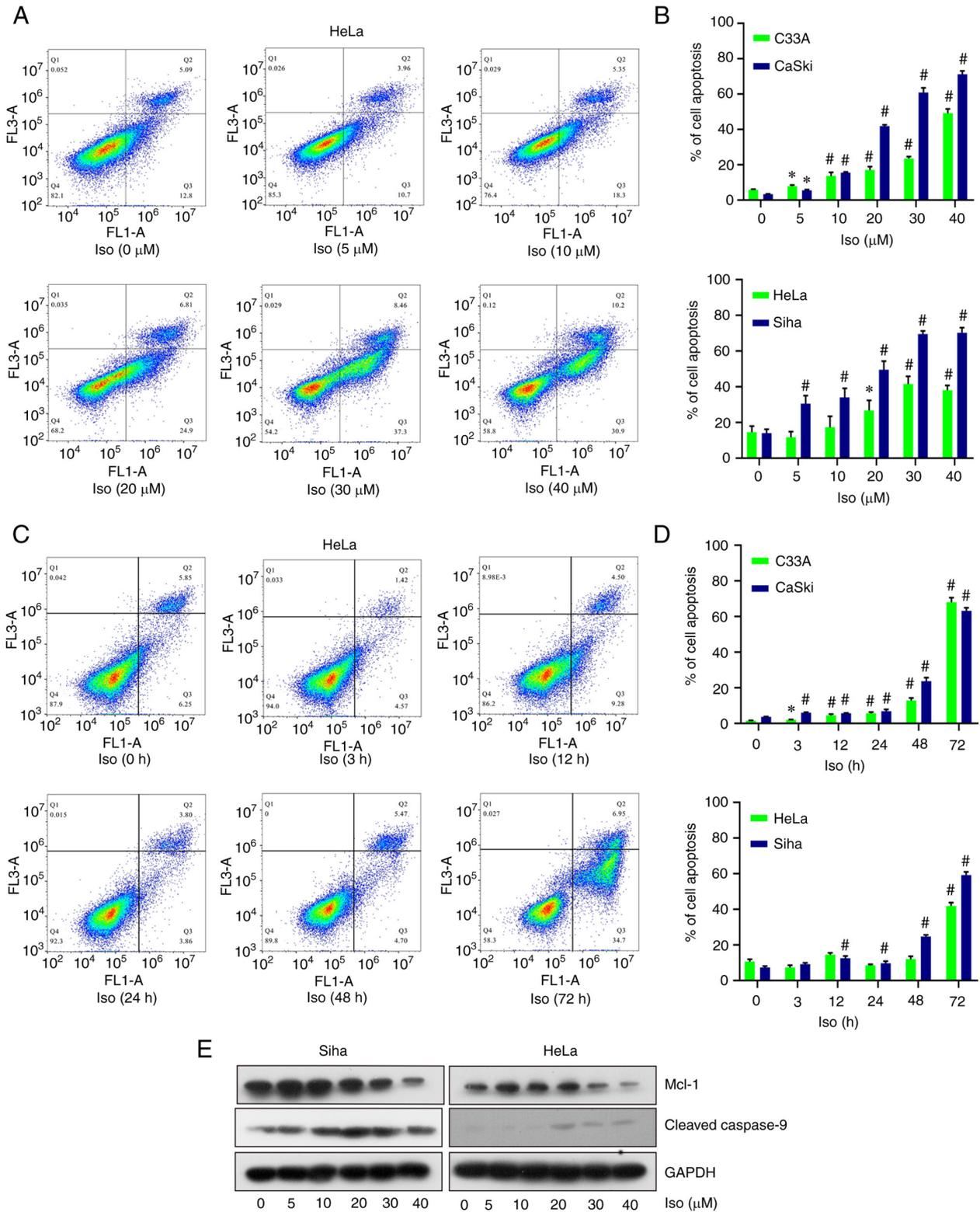
Figure 4. Isoliensinine induces cervical cancer cell apoptosis. (A) PI/Annexin V-FITC staining analysis of cell apoptosis in HeLa cells treated with 0, 5, 10, 20, 30 and 40 μM isoliensinine for 48 h. (B) Quantitative data of the cell apoptosis of the C33A, CaSki, HeLa and Siha cell lines after treatment with 20 μM isoliensinine for 0, 3, 12, 24, 48 and 72 h. (C) PI/Annexin V-FITC staining analysis of cell apoptosis in HeLa cells treated with 20 μM isoliensinine for 0, 3, 12, 24, 48 and 72 h. (D) Quantitative data of the cell apoptosis of the C33A, CaSki, HeLa and Siha cell lines after treatment with 20 μM isoliensinine for 0, 3, 12, 24, 48 and 72 h. (E) Western blot analysis of Mcl-1 and cleaved caspase-9 protein levels in HeLa and SiHa cells treated with 0, 5, 10, 20, 30 and 40 μM isoliensinine for 48 h. GAPDH was used as control. $^*P<0.05$ and $^\#P<0.01$ vs. 0 (Further data are included in Figs. S3-S5). Iso, isoliensinine; Mcl-1, myeloid-cell leukemia 1.

To investigate if cell cycle arrest and apoptosis induced by isoliensinine and AKTi-1/2 co-treatment were related to the AKT/GSK3α pathway, the expression of AKT, phosphorylation of AKT (S473), GSK3α and p21 were measured. After treatment with isoliensinine and/or AKTi-1/2, the expression of GSK3α was decreased whilst
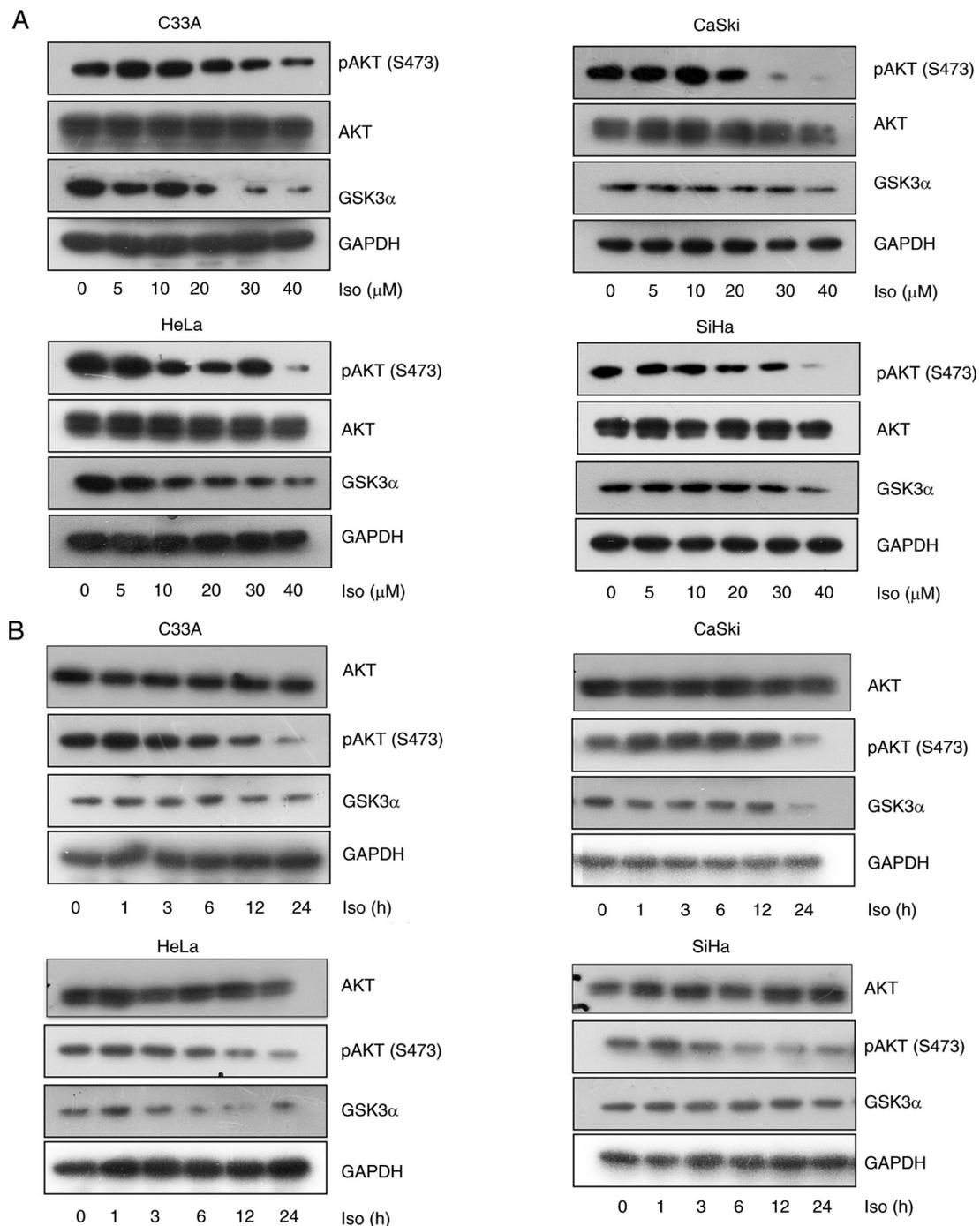
Figure 5. Isoliensinine inhibits AKT (S473) phosphorylation and GSK3α expression. Western blotting of AKT, p-AKT (S473) and GSK3α in C33A, CaSki, HeLa and SiHa cervical cancer cells treated with (A) 0, 5, 10, 20, 30 and 40 μM isoliensinine for 24 h or (B) 20 μM isoliensinine for 0, 1, 3, 6, 12 and 24 h. GAPDH was used as a control. Iso, isoliensinine; p-, phosphorylated; GSK3α, glycogen synthase kinase 3α.

the expression of p21 was increased in cervical cancer cells (Fig. 8E). Taken together, these data suggest that AKTi-1/2 potentiated the function of isoliensinine to induce cervical cancer cell cycle arrest and apoptosis through the AKT/GSK3α pathway in cervical cancer cells, which appeared to be an 'additive' effect.

Discussion

Isoliensinine is a naturally occurring compound and a bisbenzylisoquinoline alkaloid that can be isolated from the lotus plant *Nelumbo nucifera* Gaertn (16). Although previous studies have demonstrated a variety of therapeutic effects of isoliensinine, including antioxidant, antiaging and anticancer effects (14-16), this compound has not been explored in-depth. Therefore, the present study investigated the mechanism underlying the effects of isoliensinine on cell cycle arrest and apoptosis in cervical cancer cells. The results revealed that isoliensinine markedly inhibited cell proliferation by inducing cell cycle arrest and apoptosis, which was likely the result of AKT/GSK3α pathway inhibition.
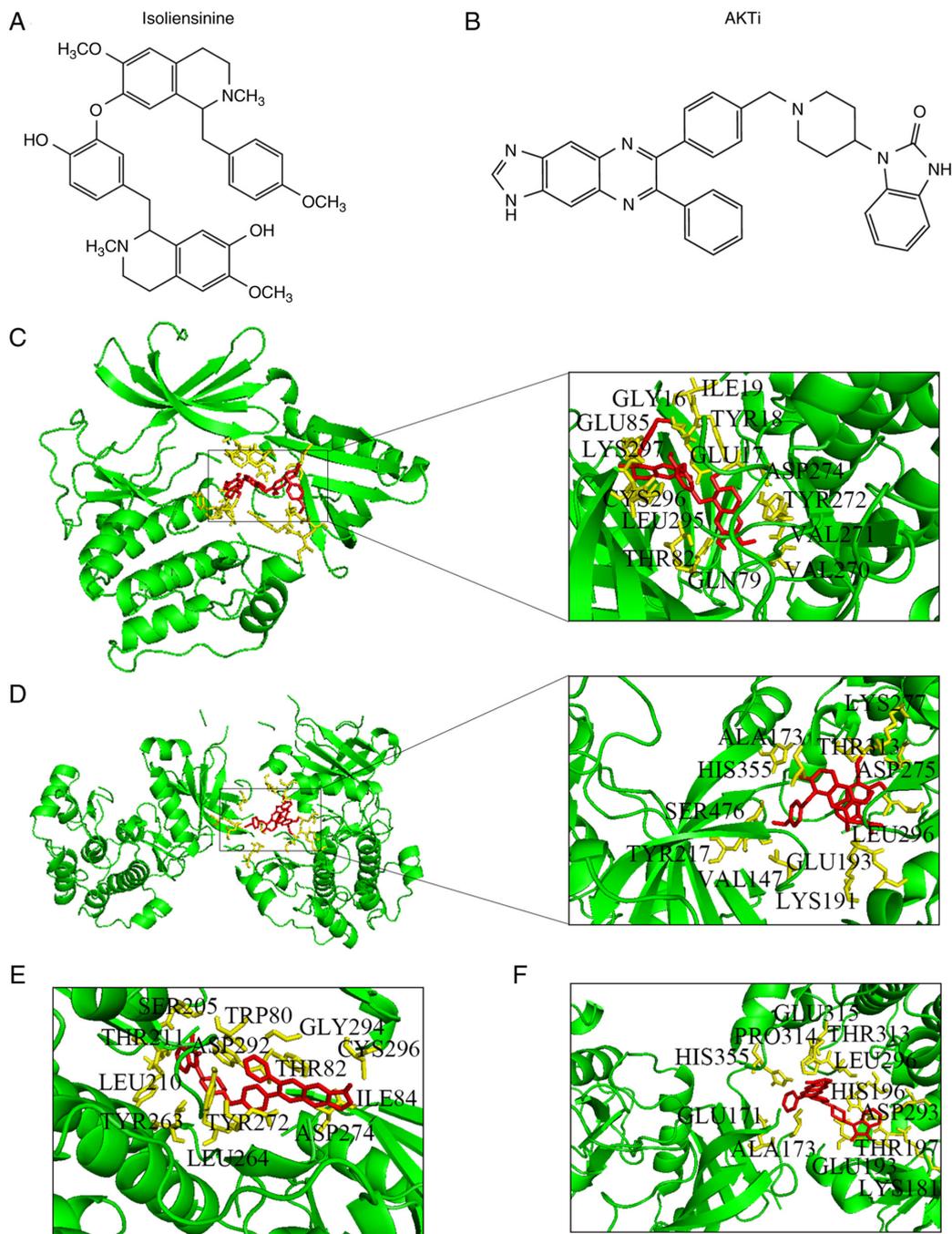
Figure 6. Docking of isoliensinine and AKTi-1/2 into AKTs. Chemical structures of (A) isoliensinine and (B) AKTi-1/2. Isoliensinine bound to (C) AKT1 and (D) AKT2. AKTi-1/2 bound to (E) AKT1 and (F) AKT2.

Cell cycle arrest is a method of eliminating cancer cells, where previous studies have found that isoliensinine can inhibit the proliferation of colorectal and breast cancer cells (16,19). Interestingly, CCK-8 assay results showed that HPV16/18 double-positive Caski cells and HPV-negative C33A cells were more sensitive to isoliensinine compared with the HPV16/18 single-positive HeLa and SiHa cells. Similar results were also found in hepatitis B virus-negative HepG2 cells (16). Therefore, it could be concluded that isoliensinine can exert inhibitory effects on the proliferation of cervical cancer cells independent of HPV. In addition, isoliensinine was found to inhibit cervical cancer cell proliferation by upregulating p21 expression whilst inducing cell

cycle arrest at the G_0/G_1 checkpoint. Similarly, a previous study found that isoliensinine can induce cell cycle arrest at the G_1 phase by also upregulating p21 expression in breast cancer cells (19). Therefore, this suggests that isoliensinine can inhibit cell proliferation through induction of cell cycle arrest.

Mechanistically, isoliensinine was found to downregulate CDK2 and cyclin E expression in cervical cancer cells. After CDK2 and cyclin E expression was downregulated, the cell cycle was not able to progress into the S or G_2/M phases, instead being arrested at the G_0/G_1 phase (8,9). p21 binds to the CDK2/cyclin E complex, thereby preventing the cell cycle from entering S phase (8,9). Therefore, a decreased cell

11
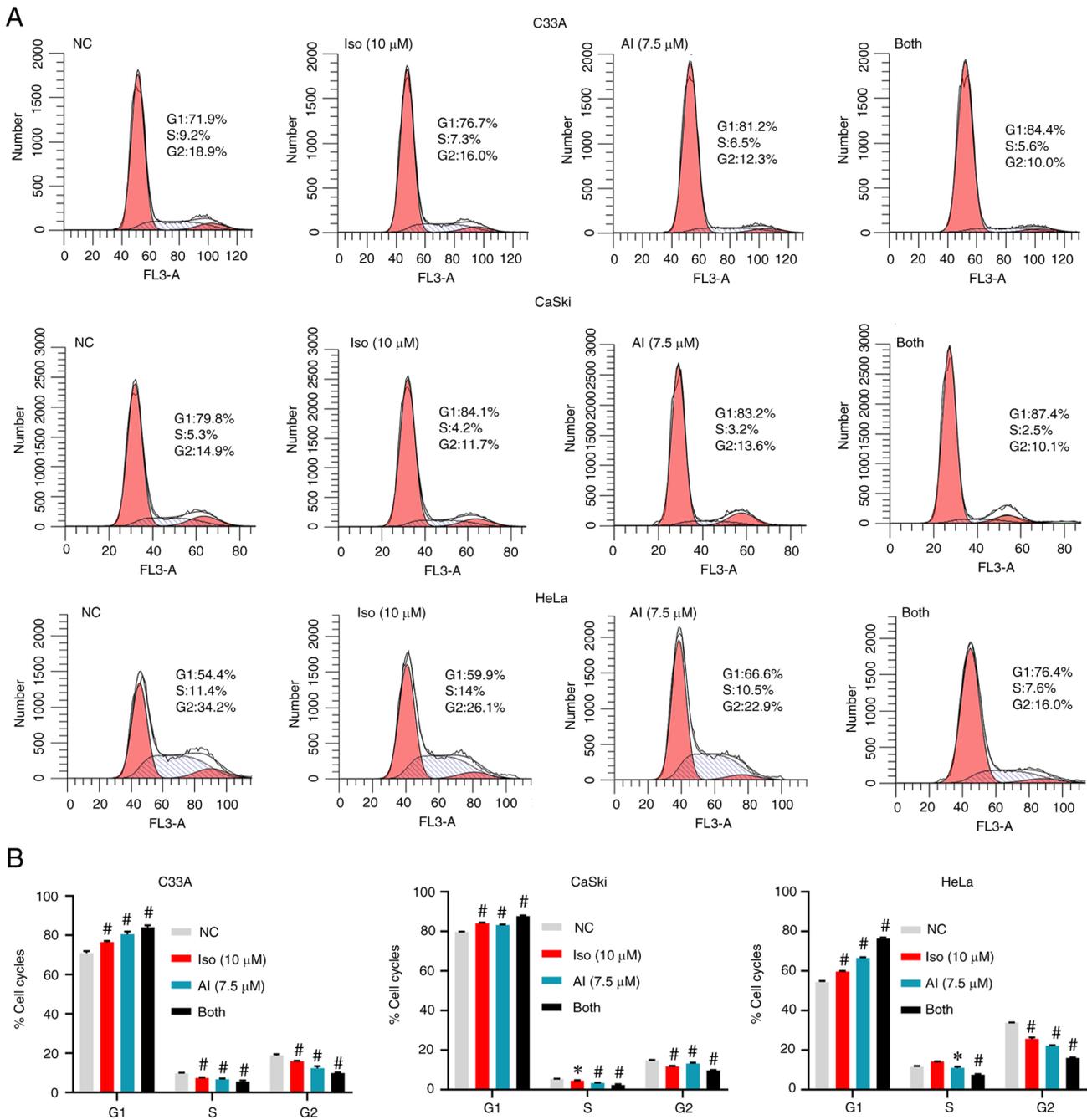
Figure 7. AKTi-1/2 enhances the function of isoliensinine to inhibit cervical cancer cell proliferation. The cells were treated with isoliensinine (10 μM) and/or AKTi-1/2 (7.5 μM) for 24 h. In total, 0.1% DMSO was used as a negative control. (A) Cell cycle distribution of C33A, CaSki and HeLa cervical cancer cells. (B) Quantitative data of C33A, CaSki and HeLa cervical cancer cell cycle distribution. *P<0.05 and #P<0.01 vs. NC group. NC, negative control; Iso, isoliensinine; AI, AKTi-1/2.

distribution in the S and G_2/M phases and an increase in G_0/G_1 phase were observed.

Subsequently, it was observed that isoliensinine inhibited cell cycle progression by downregulating AKT phosphorylation and GSK3α expression. However, isoliensinine did not alter the expression of PTEN, which is the negative regulator of Akt. These data are different from previous findings, which showed that isoliensinine can upregulate p21 through the MAPK/JNK pathway in breast cancer cells (18). Taken together, these results suggest that isoliensinine may have multiple targets when exerting antitumor proliferation effects.

Basal AKT activity was previously found to be generally high in cervical cancer cells (4,7). In the present study, it was significantly inhibited by isoliensinine in a dose- and time-dependent manner. Previous studies have shown that AKTi-1/2 can downregulate GSK3α whilst upregulating p21 to induce cell cycle arrest at the G_0/G_1 phase in ovarian cancer cells and chronic lymphocytic leukemia cells (32,33). Similarly, the present study also revealed that p21 expression was increased after isoliensinine or AKTi-1/2 treatments. Therefore, isoliensinine inhibits cervical cancer cell cycle arrest through the AKT/GSK3α/p21 pathway.
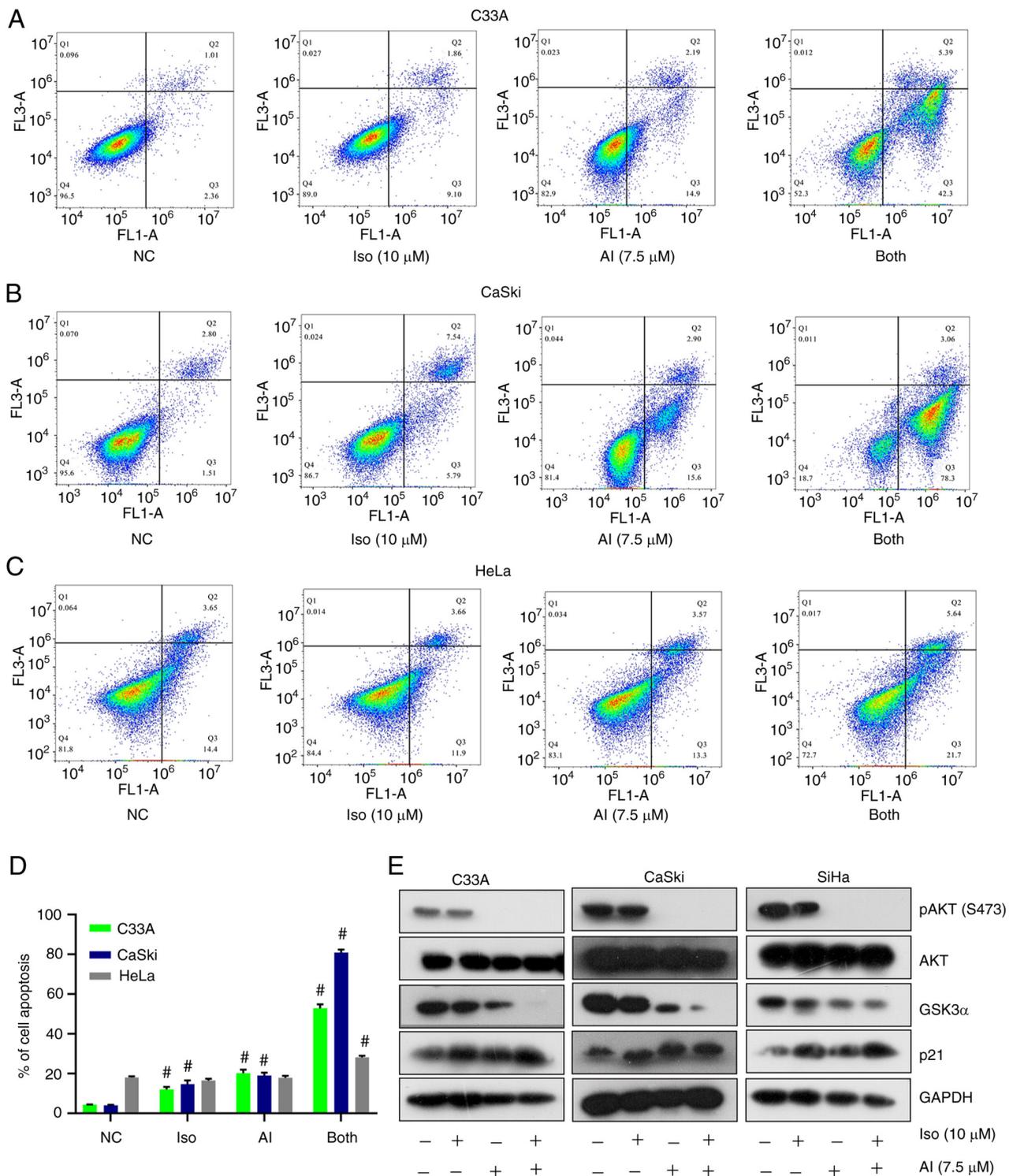
Figure 8. AKTi-1/2 enhances the function of isoliensinine to induce cervical cancer cell apoptosis. PI/Annexin V-FITC staining analysis of cell apoptosis in (A) C33A, (B) CaSki and (C) HeLa cells after they were treated with isoliensinine (10 μM) and/or AKTi-1/2 (7.5 μM) for 48 h. (D) Quantitative data of C33A, CaSki and HeLa cervical cancer cell apoptosis. (E) Western blot analysis of AKT, p-AKT (S473), GSK3α and p21 levels in cervical cancer cells treated with isoliensinine (10 μM) and/or AKTi-1/2 (7.5 μM) for 24 h. GAPDH was used as a control. [#]P<0.01 vs. NC group. NC, negative control; Iso, isoliensinine; AI, AKTi-1/2; p-, phosphorylated.

In terms of apoptosis, the present study showed that isoliensinine can inhibit cell proliferation by inducing cell apoptosis in cervical cancer cell apoptosis through the AKT/GSK3α/Mcl-1 pathway. However, previous reports reported that isoliensinine induces cancer cell apoptosis through the NF-κB/Bcl-2 cascade in hepatocellular carcinoma cells and the MAPK/Bcl-2 cascade

in breast cancer cells (17,18). Furthermore, the present study showed that AKTi-1/2 or isoliensinine can induce cervical cancer cell apoptosis but exerted seemingy additive effects when combined. During the dose selection of AKTi-1/2, only observation of cell death at the corresponding doses was used in the methodology, which is a limitation of the present

study. A previous study found that AKTi-1/2 can induce cell apoptosis by downregulating Mcl-1 expression in leukemic cells (34). Therefore, the mechanism by which isoliensinine induces apoptosis in cervical cancer cells may be similar to that by AKTi-1/2. To conclude, isoliensinine induces cervical cancer cell apoptosis in a caspases-dependent manner.

GSK3α is negatively regulated by AKT (7). However, the present study found that isoliensinine or AKTi-1/2 down-regulated AKT phosphorylation, which negatively regulated GSK3α. A previous study found that GSK3α expession is positively regulated by AKT during cell cycle arrest and apoptosis in A549, MCF-7 and HepG2 cells (35). GSK3α can be directly or indirectly regulated by AKT after isoliensinine treatment in cancer cells, which warrants further investigation. Subsequent docking analysis showed that the docking mechanism of isoliensinine onto AKT1/2 was similar to that of AKTi-1/2. Therefore, isoliensinine can directly inhibit AKT by direct interaction, which may serve to be a novel direction for cervical cancer treatment.

AKTi-1/2 is an allosteric inhibitor that can bind to AKT between the PH domain and the kinase domain (36). The PH domain is regulated by PI3K, which releases the kinase domain to be phosphorylated by phosphoinositide-dependent kinase-1 in AKT1 (7). In the present study, the binding site of isoliensinine was similar to that of AKTi-1/2 with AKT protein. The downregulation of AKT phosphorylation was likely exerted by binding to AKT. Additionally, western blot analysis showed that isoliensinine did not affect AKTi-1/2 binding to AKT. Furthermore, isoliensinine-targeted AKT reduced AKT phosphorylation. However, this mechanism remains to be elucidated by pull-down and kinase assays.

In summary, the present study confirmed that isoliensinine can regulate the AKT/GSK3α signaling pathway to inhibit cell proliferation whilst inducing the apoptosis of cervical cancer cells *in vitro*. However, the lack of *in vivo* experiments is a limitation of the present study. Additionally, patients with cervical cancer typically present at advanced stages (1). The main treatment methods for these patients include chemotherapy, radiotherapy and combined chemoradiotherapy (37). Compared with chemotherapy, radiotherapy has advantages of low toxicity, superior efficacy, abilities of local targeting and whole course treatment (37). The isoliensinine compound alone was found to exert beneficial effects by inducing apoptosis whilst inhibiting the proliferation of the cervical cancer cell lines. Therefore, the potential advantages and disadvantages of akt inhibition and/or radiotherapy alone or in combination for patients with cervical cancer should be explored in th future.

Collectively, the present study identified the impact of isoliensinine-mediated inhibition on cervical cancer cell proliferation, which was by inducing cell cycle arrest and apoptosis. Cell cycle arrest was likely induced by upregulating p21 expression whilst downregulating that of CDK2 and cyclin E. By contrast, cell apoptosis is mediated by decreasing Mcl-1 expression and activating of caspase-9. Furthermore, the mechanisms of action underlying the effects of isoliensinine on cell cycle arrest and apoptosis om cervical cancer cells are likely associated with AKT phosphorylation inhibition and GSK3α downregulation. Therefore, isoliensinine likely induces cervical cancer cell cycle arrest and apoptosis by

inhibiting the AKT/GSK3α pathway. Isoliensinine may be a novel AKT inhibitor for the treatment of cervical cancer.

Acknowledgements

Funding

Availability of data and materials

The datasets used and/or analyzed during the current study are available from the corresponding author on reasonable request.

Authors' contributions

HLL and YC designed the study and performed the experiments. ZWZ, HZL and HYL helped to perform the experiments. DDW, LC and LCG contributed to the conception and design of the work. In addition, LC critically revised the manuscript and LCG approved the version to be published. All authors read and approved the final version of the manuscript. HLL, YC and LCG confirm the authenticity of all the raw data.

Ethics approval and consent to participate

Not applicable.

Patient consent for publication

Not applicable.

Competing interests

The authors declare that they have no competing interests.

References

1. Sung H, Ferlay J, Siegel RL, Laversanne M, Soerjomataram I, Jemal A and Bray F: Global cancer statistics 2020: GLOBOCAN estimates of incidence and mortality worldwide for 36 cancers in 185 countries. CA Cancer J Clin 71: 209-249, 2021.
2. Šarenac T and Mikov M: Cervical cancer, different treatments and importance of bile acids as therapeutic agents in this disease. Front Pharmacol 10: 484, 2019.
3. Zhang L, Wu J, Ling MT, Zhao L and Zhao KN: The role of the PI3K/Akt/mTOR signalling pathway in human cancers induced by infection with human papillomaviruses. Mol Cancer 14: 87, 2015.

4. Kim TJ, Lee JW, Song SY, Choi JJ, Choi CH, Kim BG, Lee JH and Bae DS: Increased expression of pAKT is associated with radiation resistance in cervical cancer. Br J Cancer 94: 1678-1682, 2006.
5. Balasuriya N, McKenna M, Liu X, Li SS and O'Donoghue P: Phosphorylation-dependent inhibition of Akt1. Genes (Basel) 9: 450, 2018.
6. Manning BD and Toker A: AKT/PKB signaling: Navigating the network. Cell 169: 381-405, 2017.
7. Shi X, Ran L, Liu Y, Zhong SH, Zhou PP, Liao MX and Fang W: Knockdown of hnRNP A2/B1 inhibits cell proliferation, invasion and cell cycle triggering apoptosis in cervical cancer via PI3K/AKT signaling pathway. Oncol Rep 39: 939-950, 2018.
8. Manning BD and Cantley LC: AKT/PKB signaling: Navigating downstream. Cell 129: 1261-1274, 2007.
9. Zhuang J, Hawkins SF, Glenn MA, Lin K, Johnson GG, Carter A, Cawley JC and Pettitt AR: Akt is activated in chronic lymphocytic leukemia cells and delivers a pro-survival signal: The therapeutic potential of Akt inhibition. Haematologica 95: 110-118, 2010.
10. Karimian A, Ahmadi Y and Yousefi B: Multiple functions of p21 in cell cycle, apoptosis and transcriptional regulation after DNA damage. DNA Repair (Amst) 42: 63-71, 2016.
11. Liu J, Li Q, Liu Z, Lin L, Zhang X, Cao M and Jiang J: Harmine induces cell cycle arrest and mitochondrial pathway-mediated cellular apoptosis in SW620 cells via inhibition of the Akt and ERK signaling pathways. Oncol Rep 35: 3363-3370, 2016.
12. Behan FM, Iorio F, Picco G, Gonçalves E, Beaver CM, Migliardi G, Santos R, Rao Y, Sassi F, Pinnelli M, *et al*: Prioritization of cancer therapeutic targets using CRISPR-Cas9 screens. Nature 568: 511-516, 2019.
13. Sharma BR, Gautam LN, Adhikari D and Karki R: A comprehensive review on chemical profiling of nelumbo nucifera: Potential for drug development. Phytother Res 31: 3-26, 2017.
14. Shen CY, Jiang JG, Yang L, Wang DW and Zhu W: Anti-ageing active ingredients from herbs and nutraceuticals used in traditional Chinese medicine: Pharmacological mechanisms and implications for drug discovery. Br J Pharmacol 174: 1395-1425, 2017.
15. Manogaran P, Beeraka NM, Huang CY and Vijaya Padma V: Neferine and isoliensinine enhance 'intracellular uptake of cisplatin' and induce 'ROS-mediated apoptosis' in colorectal cancer cells-A comparative study. Food Chem Toxicol 132: 110652, 2019.
16. Shu G, Yue L, Zhao W, Xu C, Yang J, Wang S and Yang X: Isoliensinine, a bioactive alkaloid derived from embryos of nelumbo nucifera, induces hepatocellular carcinoma cell apoptosis through suppression of NF-κB signaling. J Agric Food Chem 63: 8793-8803, 2015.
17. Law BY, Chan WK, Xu SW, Wang JR, Bai LP, Liu L and Wong VK: Natural small-molecule enhancers of autophagy induce autophagic cell death in apoptosis-defective cells. Sci Rep 4: 5510, 2014.
18. Zhang X, Wang X, Wu T, Li B, Liu T, Wang R, Liu Q, Liu Z, Gong Y and Shao C: Isoliensinine induces apoptosis in triple-negative human breast cancer cells through ROS generation and p38 MAPK/JNK activation. Sci Rep 5: 12579, 2015.
19. Livak KJ and Schmittgen TD: Analysis of relative gene expression data using real-time quantitative PCR and the 2(-Delta Delta C(T)) method. Methods 25: 402-408, 2001.
20. Baydoun HH, Pancewicz J, Bai X and Nicot C: HTLV-I p30 inhibits multiple S phase entry checkpoints, decreases cyclin E-CDK2 interactions and delays cell cycle progression. Mol Cancer 9: 302, 2010.
21. Zhang C, Xu B, Lu S, Zhao Y and Liu P: HN1 contributes to migration, invasion, and tumorigenesis of breast cancer by enhancing MYC activity. Mol Cancer 16: 90, 2017.
22. Kong R, Zhang EB, Yin DD, You LH, Xu TP, Chen WM, Xia R, Wan L, Sun M, Wang ZX, *et al*: Long noncoding RNA PVT1 indicates a poor prognosis of gastric cancer and promotes cell proliferation through epigenetically regulating p15 and p16. Mol Cancer 14: 82, 2015.
23. Xin X, Wu M, Meng Q, Wang C, Lu Y, Yang Y, Li X, Zheng Q, Pu H, Gui X, *et al*: Long noncoding RNA HULC accelerates liver cancer by inhibiting PTEN via autophagy cooperation to miR15a. Mol Cancer 17: 94, 2018.
24. Weisner J, Landel I, Reintjes C, Uhlenbrock N, Trajkovic-Arsic M, Dienstbier N, Hardick J, Ladigan S, Lindemann M, Smith S, *et al*: Preclinical efficacy of covalent-allosteric AKT inhibitor borussertib in combination with trametinib in *KRAS*-Mutant pancreatic and colorectal cancer. Cancer Res 79: 2367-2378, 2019.
25. Heerding DA, Rhodes N, Leber JD, Clark TJ, Keenan RM, Lafrance LV, Li M, Safonov IG, Takata DT, Venslavsky JW, *et al*: Identification of 4-(2-(4-amino-1,2,5-oxadiazol-3-yl)-1-ethyl-7-{[(3S)-3-piperidinylmethyl]oxy}-1H-imidazo[4,5-c]pyridin-4-yl)-2-methyl-3-butyn-2-ol (GSK690693), a novel inhibitor of AKT kinase. J Med Chem 51: 5663-5679, 2008.
26. Salony, Solé X, Alves CP, Dey-Guha I, Ritsma L, Boukhali M, Lee JH, Chowdhury J, Ross KN, Haas W, *et al*: AKT inhibition promotes nonautonomous cancer cell survival. Mol Cancer Ther 15: 142-153, 2016.
27. Kadioglu O, Law BY, Mok SW, Xu SW, Efferth T and Wong VK: Mode of action analyses of neferine, a bisbenzylisoquinoline alkaloid of lotus (*Nelumbo nucifera*) against multidrug-resistant tumor cells. Front Pharmacol 8: 238, 2017.
28. Zhang T, Zhao C, Luo L, Zhao H, Cheng J and Xu F: The expression of Mcl-1 in human cervical cancer and its clinical significance. Med Oncol 29: 1985-1991, 2012.
29. Cuconati A, Mukherjee C, Perez D and White E: DNA damage response and MCL-1 destruction initiate apoptosis in adenovirus-infected cells. Genes Dev 17: 2922-2932, 2003.
30. Zhang Q, Yang M, Qu Z, Zhou J and Jiang Q: Autophagy prevention sensitizes AKTi-1/2-induced anti-hepatocellular carcinoma cell activity in vitro and in vivo. Biochem Biophys Res Commun 480: 334-340, 2016.
31. Correa RJ, Valdes YR, Peart TM, Fazio EN, Bertrand M, McGee J, Préfontaine M, Sugimoto A, DiMattia GE and Shepherd TG: Combination of AKT inhibition with autophagy blockade effectively reduces ascites-derived ovarian cancer cell viability. Carcinogenesis 35: 1951-1961, 2014.
32. Fekete M, Santiskulvong C, Eng C and Dorigo O: Effect of PI3K/Akt pathway inhibition-mediated G1 arrest on chemosensitization in ovarian cancer cells. Anticancer Res 32: 445-452, 2012.
33. de Frias M, Iglesias-Serret D, Cosialls AM, Coll-Mulet L, Santidrián AF, González-Gironès DM, de la Banda E, Pons G and Gil J: Akt inhibitors induce apoptosis in chronic lymphocytic leukemia cells. Haematologica 94: 1698-1707, 2009.
34. Prabhu KS, Siveen KS, Kuttikrishnan S, Jochebeth A, Ali TA, Elareer NR, Iskandarani A, Quaiyoom Khan A, Merhi M, Dermime S, *et al*: Greensporone A, a fungal secondary metabolite suppressed constitutively activated AKT via ROS generation and induced apoptosis in leukemic cell lines. Biomolecules 9: 126, 2019.
35. Reddy D, Ghosh P and Kumavath R: Strophanthidin attenuates MAPK, PI3K/AKT/mTOR, and Wnt/β-catenin signaling pathways in human cancers. Front Oncol 9: 1469, 2020.
36. Gilot D, Giudicelli F, Lagadic-Gossmann D and Fardel O: Akti-1/2, an allosteric inhibitor of Akt 1 and 2, efficiently inhibits CaMKIα activity and aryl hydrocarbon receptor pathway. Chem Biol Interact 188: 546-552, 2010.
37. Cohen PA, Jhingran A, Oaknin A and Denny L: Cervical cancer. Lancet 393: 169-182, 2019.